Radio Science, Volume 9, Number 11, pages 941–955, November 1974

Radio frequency scattering from a heated ionospheric volume, 1, VHF/UHF field-aligned and plasma-line backscatter measurements

J. Minkoff, P. Kugelman[1], *and I. Weissman*

Riverside Research Institute, New York, N.Y. 10023

(Received July 30, 1974.)

It is observed that an ionospheric volume in the *F* layer subjected to high power HF illumination becomes an effective scattering medium for radio signals in the VHF/UHF frequency range. The experimental results are representative of a field-aligned scattering geometry for which the first such observations of VHF/UHF scattering from a heated ionospheric volume are presented. Two distinct scattering modes are observed, center-line and plasma-line scattering. Center-line scattering is observed at the transmitted radar frequency f; plasma-line scattering is observed as a pair of sidebands at $f \pm f_h$ where f_h is the heater frequency. The two scattering modes are observed to have markedly dissimilar characteristics. Center-line scattering is highly aspect sensitive with respect to the direction of the geomagnetic field, **B**; plasma-line scattering is found to be much less aspect sensitive, if at all. The region of maximum backscatter for the center-line mode is found from these measurements to consist of the locus of points within the heated volume over which perpendicularity between the radar line of sight and **B** is achieved, independent of the location of maximum heating. The backscattering region for the plasma-line mode is found from these measurements to be determined by the altitude of maximum heating, independent of geometrical considerations involving **B**. The longitudinal coherence length, L, for center-line scattering is found from these measurements to be greater than the maximum antenna diameter of 85 ft; no more exact estimate for L is possible. A striking reversal in frequency dependence is found between the center-line and plasma-line modes. The per-unit-volume center-line backscatter cross section is found to be about 7 db greater at VHF than at UHF; the per-unit-volume plasma-line backscatter cross section is found to be at least 11 db less at VHF than at UHF. Preliminary results concerning time-dependent behavior are presented. For both modes the scattering cross section is found to be effectively turned on and off very rapidly in response to the heater excitation; the spectral width of the scattering for both modes is found to be quite narrow (about 10 Hz). The spatial configuration of the heated volume is investigated; significant differences are observed depending on whether f_h/f_oF_2 is greater or less than unity.

1. INTRODUCTION

This paper reports the first observations of radar backscatter in the VHF/UHF frequency range from a heated ionospheric volume. The ionospheric heating, by means of high power illumination in the HF range using a 10-element circular array located at Platteville, Colorado, was performed by the Institute for Telecommunication Sciences (ITS) under the direction of W. F. Utlaut [*Utlaut*, 1970; *Carroll et al.*, 1974; *Utlaut and Violette*, 1974]. *o*-mode heating was used predominantly throughout these experiments, and the heating frequencies ranged nominally between 3 and 10 MHz. Maximum heating takes place at the reflection altitude of the HF wave where the group velocity of the heating signal goes to zero; at this altitude, h_r, the heating frequency, f_h, is equal to the local plasma frequency f_p. The radars used in these experiments were located at the White Sands Missile Range (WSMR), for which the experimental geometry is shown in Figure 1. The magnetic declination and dip angle at the heater are 13° and 68°, respectively. The azimuthal bearing from the nominal location of the WSMR radars to the Platteville heater is 8° with the line of sight therefore lying very nearly within the magnetic meridian plane; for a 15° radar elevation angle at White Sands, the line of sight achieves perpendicularity to the earth's magnetic field, **B**, at a point above the heater at an altitude of about 290 km. This geometry therefore represents a nearly ideal situation for field-

[1] Present address: E. I. Dupont De Nemours & Co., Martinsville, Va. 24112.

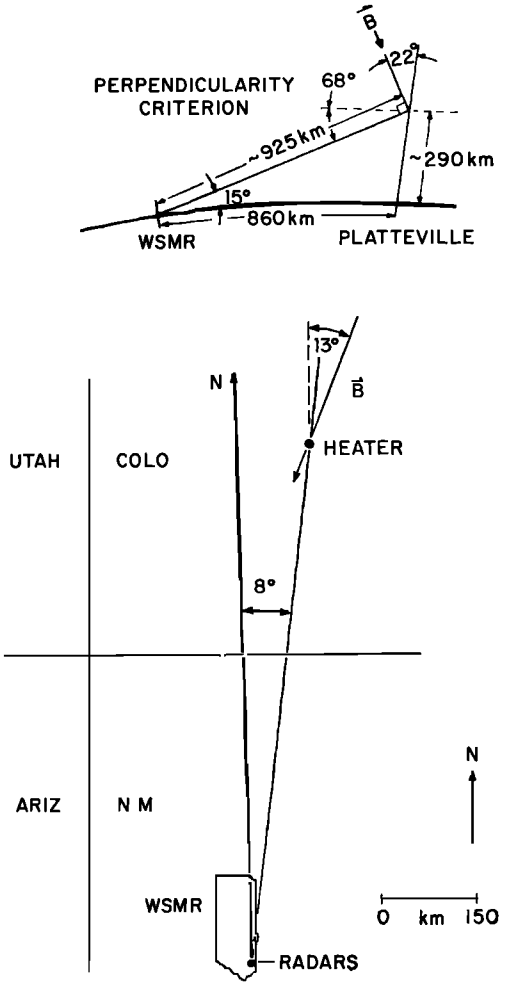

Fig. 1. White Sands—Platteville experiment geometry. The azimuthal heading between the radars at White Sands and the heater is 8°. The magnetic dip angle at Platteville is 68° and the declination is 13°. For a 15° radar elevation angle, the line of sight is perpendicular to B above the heater at an altitude of about 290 km.

aligned scattering measurements in the *F* layer, for which the first such observations in the VHF/UHF frequency range as a result of the effects of ionospheric heating were obtained during these experiments in early June 1971.

Experimental results for two distinct and markedly dissimilar scattering modes are presented. For the first mode, referred to as center-line scattering, the frequency of the received signal is essentially the same as the frequency of the transmitted signal, f, aside from perhaps a small Doppler shift due to ionospheric drift. These observations can be understood in terms of scattering from turbulence in the ionospheric electron density distribution which, for purposes of scattering at these wavelengths—1.9 and .69 m—is observed to be effectively turned on and off quite rapidly in response to the HF heater excitation. For this mode of scattering a number of interesting similarities to the radio aurora are observed. As was first determined from bistatic measurements described by *Minkoff et al.* [1974], center-line scattering takes place from long columns of ionization aligned with **B**. All experimental observations, those presented below as well as other measurements at different locations and frequencies [*Fialer*, 1974; *Carpenter*, 1974] show without exception that this mode of scattering is highly aspect sensitive with respect to the direction of **B**, and can be described in terms of a specular reflection of the transmitted signal off the magnetic field lines, the angle of incidence being equal to the angle of reflection, with, as a special case, perpendicular incidence to **B** being required for backscatter. Thus, for the center line, scattering from one location to another takes place from a prescribed region which is completely specified by the geometry relative to **B**, independent of the heating altitude h_f.

In order to have a quantitative measure of the aspect sensitivity it is convenient to speak in terms of a longitudinal scale size, L [*Booker*, 1956], defined such that the angular width of the scattering lobe is of the order of λ/L, where λ is the radar wavelength; the quantity L is a measure of the average length of the field-aligned scattering structures. However, because of fundamental limitations imposed by the spatial resolution capabilities of the radar system on the extent to which this quantity can actually be determined [*Minkoff*, 1973*a*, *b*], it was possible to conclude only that a representative value of L for these experiments is larger, and probably significantly larger, than the maximum antenna diameter which was 85 ft. From the center-line measurements at these two frequencies it was also found that the per-unit-volume backscatter cross section at VHF (157.5 MHz) exceeds that at UHF (435 MHz) by approximately 7 db [*Minkoff*, 1974].

The second scattering mode appears as a pair of side bands displaced by $\pm f_h$ on either side of the center-line signal, as for example would occur if the center-line cross section were sinusoidally amplitude modulated at a frequency f_h, and was observed by detuning the receiver to $f \pm f_h$; no scattering was observed at $f \pm 2f_h$, $f \pm 3f_h$, $\cdots$. It should be pointed out that knowledge of the exact frequency offsets of the returns for this scattering mode was limited by the receiver bandwidths used in these experiments which

were 30 and 100 kHz at VHF and UHF, respectively. This mode has been denoted as plasma-line scattering because of the similarity with regard to the characteristic frequency offsets to results which have been reported at the Arecibo Ionospheric Observatory (AIO) [*Yngvesson and Perkins*, 1968; *Gordon and Carlson*, 1974; *Wong and Taylor*, 1971]. For the AIO observations however, the spectral widths of the returns are found to be of the order of 2 kHz whereas for the plasma-line echoes for the field-aligned geometry in these experiments the spectral widths have been found to be of the order of 10 Hz which is extremely narrow band in comparison. Furthermore, existing theories [*Perkins et al.*, 1974] which explain the generation of plasma waves in terms of parametric instabilities produced by the heating, and which have been quite successful in calculating the spectra of the plasma-line echoes observed at AIO, also predict that for *o*-mode heater excitation, which applies to all these plasma-line results, such waves propagate within a 10° to 20° cone centered on **B**. For the geometry of the White Sands experiments however, the experimental results require waves propagating normal to **B**, and it would therefore seem that these theories do not apply. Hence it is not known at this time whether the second scattering mode observed in these experiments was actually produced by plasma waves resulting from parametric instabilities or by some other mechanism.

For the field-aligned geometry, the first such plasma-line scattering resulting from the heating process was observed at White Sands in January 1972. In addition to being dissimilar to the AIO plasma-line observations, this scattering mode also differs significantly from center-line scattering with regard to the definition of the location of the scattering region and the aspect sensitivity, as well as the frequency dependence of the backscatter cross section. With regard to definition of the location of the scattering region, in contrast to the center-line mode, plasma-line scattering was found invariably to be maximized by directing the radar line-of-sight to the nominal altitude where the maximum HF heating was believed to be taking place, independent of geometrical considerations concerning **B**. This indicates, at the least, a much weaker aspect sensitivity for plasma-line scattering, which was borne out in observations where plasma-line backscatter was observed for h_f values in the vicinity of 200 km, for which the angle of incidence to **B** above the heater was about 5° (for line of sight perpendicular to **B** the angle of incidence is zero). For angles of incidence to **B** as large as this, center-line backscattering was never observed. However, since maximum plasma-line echoes were observed for $h_f \simeq 290$ km, at which altitude the line of sight is nominally perpendicular to **B** above the heater, the possibility cannot be ruled out that the plasma-line scattering may be aspect sensitive to some extent. This question was not resolved by these experiments.

The frequency dependence of the backscatter cross section was also found to differ significantly between the center-line and plasma-line scattering. In the former case, at VHF, the backscattered power was of the order of 25 db (±3 db) greater than for the plasma line, whereas at UHF the received power for both scattering modes was found to be essentially the same. As is noted above, for the center line the per-unit-volume backscatter cross section was approximately 7 db greater at VHF than at UHF; however, for the plasma line, the per-unit-volume backscatter cross section is estimated here from these results to have been at least 11 db *less* at VHF than at UHF. This represents a striking reversal in the frequency dependence between the center-line and plasma-line scattering properties of the heated ionospheric volume.

The major similarity between the two modes was observed with regard to their time-dependent behavior. The scattering in both cases was found to be characterized by extremely rapid rise and decay times as well as narrow spectral widths.

The experimental results presented below were obtained between June 1971 and September 1973. A list of the different WSMR sensors that were used in these experiments, together with their relevant characteristics, is presented in Table 1; a list of experiments showing the different times of the year during which the observations were made is presented in Table 2. Positive results were obtained at VHF and UHF only, using the multifrequency RAM and RTMS radars. All the WSMR radars were sufficiently close to one another (< 15 km), and the slant range to the heated volume sufficiently great, that differences in the lines of sight to the heated volume from different radars for a given azimuth and elevation angle can be ignored. The RAM radar, at VHF only, had a coherent recording capability by means of which the center-line and plasma-line spectra referred to above were obtained. Because of the narrow antenna beams these radars were also well suited for examining the spatial configuration of the heated volume under various conditions, for which

TABLE 1. Radar parameters.

Sensor	Frequency (MHz)	Peak power (Mw)	Maximum pulse width (μsec)	PRF (sec^{-1})	Antenna 3-db beamwidth (deg)
			30 CW or chirp		
RAM (VHF)	157.5	10	(compressed to 0.25)	100	5.2
RAM (UHF)	435	12	10	100	2.0
AMRAD	1300	10	8	50	0.9
RAMPART	3022	16	30	100	0.4
	150.35	.390	65	73	5.2
RTMS	354.9	.065	65	73	2.5
	448.9	.065	65	73	1.7

the results presented below are particularly interesting for $f_h/f_oF_2 > 1$.

This paper is organized as follows. Section 2 presents measurements and calculations of center-line and plasma-line backscatter cross sections. Section 3 deals with the aspect sensitivity of the two scattering modes. Some results of analysis of the time-dependent behavior of the center-line and plasma-line scattering are presented in section 4. In section 5 the observations of the spatial configuration of the heated volume are presented.

2. CROSS SECTIONS

2. 1. *Center line.*

All the results in this section were obtained with the RAM radar. As noted in the preceding section, although maximum heating occurs at the altitude h_f, where the incident HF wave is reflected, the region of maximum center-line backscatter was found to be determined by the geometry relative to **B**, independent of the h_f value. Thus, regardless of where the heating was taking place, maximum backscatter was always observed for an approximate 15° radar elevation angle. Since the critical height corresponding to the *o*-mode critical frequency, f_oF_2, determined the maximum heating altitude, heating in the vicinity of the perpendicular point could be accomplished only after sundown. VHF center-line backscatter was observed at RAM whenever the h_f value was greater than or equal to about 255 km, and increased steadily as h_f increased to the perpendicular point; for $h_f \lesssim 255$ km no backscatter was observed. Thus the turbulence on the scale of the VHF wavelength (1.9 m) produced by the heating process, of sufficient magnitude to produce backscatter observable at RAM, was spread out over an altitude range of at least about 40 to 50 km above the maximum heating point. In all cases, for $h_f < 290$ km, decreasing the elevation angle in order to cause an intersection between the line of sight and the maximum heating point, and thereby destroying the perpendicular incidence above the heater between the line of sight and **B**, always resulted in a decrease of the magnitude of the backscattered center-line signal.

During most of these experiments the minimum heating frequency was about 5 MHz which, although sufficiently low to permit long nighttime heating periods in the vicinity of the perpendicular point, generally limited the maximum h_f values to about 300 km. Subsequently, installation of additional facilities at Platteville provided for a reduction in the minimum frequency to about 3 MHz, which permitted longer heating periods at higher altitudes. In general, the backscattered signal as a

TABLE 2. List of experiments. $f \pm f_h$ denotes plasma line observation, AC denotes aircraft-based receivers (see *Minkoff et al.* [1974]).

Experiment dates	Transmitting sites	Receiving sites and frequencies
June 1971	RAM	RAM—VHF/UHF
	DUCK (HF)[1]	AC—VHF/HF
July 1971	RAM	RAM—VHF/UHF
October 1971	RAM	RAM—VHF/UHF
January 1972	RAM	RAM—VHF ($f \pm f_h$)/UHF (includes *x*-mode observations at VHF)
February 1972	RAM	RAM—VHF ($f \pm f_h$)/UHF ($f \pm f_h$) AC—VHF
April-May 1972	RAM	RAM—VHF ($f \pm f_h$)/UHF ($f \pm f_h$) Santa Fe site—VHF El Centro site—VHF AC—VHF
August 1972	RTMS	RTMS—VHF/UHF
December 1972	RTMS	RTMS—VHF
February 1972	RTMS	RTMS—VHF/UHF
September 1973	RTMS	RTMS—VHF/UHF

[1] DUCK site about 10 miles east of RAM.

function of h_f did not appear to be symmetrical about the 290-km point. That is, for reported h_f values of 300 or 310 km the backscattered power was generally observed to be somewhat greater than for h_f values of 280 or 270 km. However, the reported h_f values for such observations, which are determined from ionogram records, could be obtained only approximately depending on the degree of spreading of the ionogram traces caused by the heating process [*Utlaut and Violette,* 1974].

For UHF center-line backscatter at RAM exactly the same discussion applies regarding the geometry relative to B, the required elevation angle, etc., with, however, the minimum h_f value for UHF backscatter observed to be about 270 km. Under optimum conditions, that is, 15° elevation angle, h_f about 290 km, and maximum heater power about 2 Mw CW, the VHF and UHF center-line backscattered signal power levels were observed to be quite repeatable, say to within ±3 db, over the two-year span of these experiments. A-scope presentations of typical large radar echoes are shown in Figure 2, top. By making a straightforward substitution of the peak values of the received power into the radar equation one obtains the values for σ_T shown in the figures. Although these quantities are normalized with respect to the different transmitted power levels and antenna gains, they are not properly normalized with respect to the different sizes of the RAM VHF and UHF per-pulse scattering volumes, and consequently say very little with regard to the true quantitative difference between the center-line scattering properties of the heated volume at these two frequencies. The correct normalization for determining the true per-unit-volume cross sections for aspect-sensitive scattering is complicated by the fact that, because of the aspect sensitivity, it is not clear what the actual backscattering volume is. This is discussed in detail by *Minkoff* [1973*a*], where the proper normalization for aspect-sensitive scattering is derived, and the results are then applied to these experimental measurements by *Minkoff* [1974]. The result is that, for these measurements, the per-unit-volume center-line backscatter cross section at 157.5 MHz exceeds that at 435 MHz by approximately 7 db.

All of the above results were obtained using *o*-mode heating. A single VHF/UHF backscatter experiment using *x*-mode heating was carried out in January 1972. The VHF backscatter was observed to be considerably weaker (about 20 to 25 db) and no UHF or plasma-line scattering was observed.

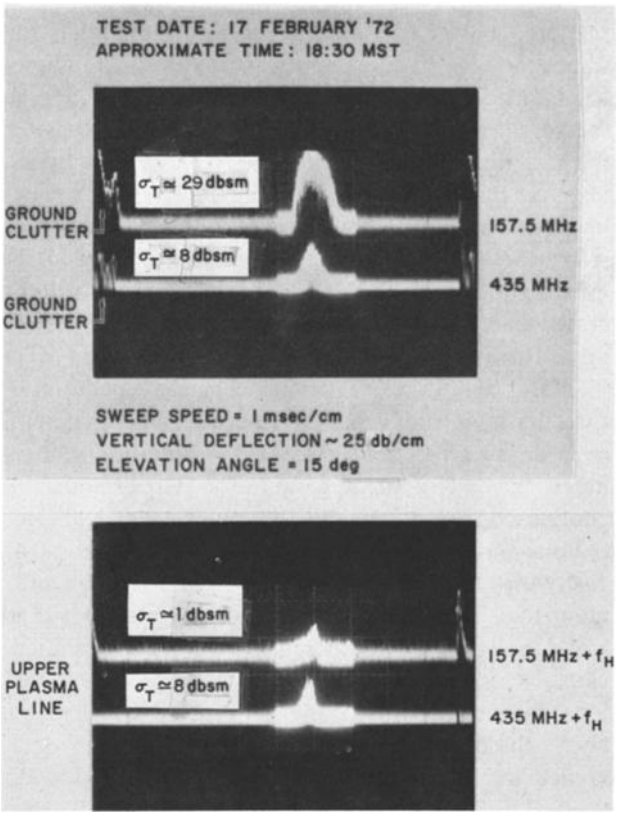

Fig. 2. A-scope presentations of typical large center-line and plasma-line radar echoes from the heated volume under optimum scattering conditions (15° RAM elevation angle, $h_f \simeq$ 290 km, heater power ≃2 Mw). The thicker base-line trace in the vicinity of the echo is due to an image intensifier in the oscilloscope. Note the absence of ground clutter in the plasma-line A-scope trace; the spikes shown on the ends of the trace represent leakage of the transmitted pulse into the receiver. σ_T is the ordinary radar cross section calculated from peak values of received power (not properly normalized with respect to per-pulse scattering volume).

2.2. *Plasma line.*

Both upper and lower plasma lines were observed, at $f + f_h$ and $f - f_h$ respectively. The backscattered power for the upper and lower plasma lines was usually found to be essentially the same, although relatively large differences (about 10 db or more) were also sometimes observed. A-scope presentations of typical large responses under optimum conditions are shown in Figure 2, bottom, for the upper plasma line; these observations were made very shortly after the center-line returns shown in Figure 2, top. It is seen that at VHF the backscattered power for the plasma-line echo is 28 db less than that for the center line, whereas at UHF the back-

scattered power for the two scattering modes is the same; the UHF pulse shapes in Figure 2 are somewhat different because, as is discussed in section 3, the scattering regions within the heated volume for the two modes are different. It is seen in Figure 2, bottom, that, without correcting for the differences between the sizes of the VHF and UHF per-pulse scattering volumes, the value of σ_T at UHF is 7 db greater than that at VHF. For the plasma-line, the correct normalization procedure in order to determine the per-unit-volume cross section is different than for center-line scattering, because in the latter case the scattering is highly aspect sensitive whereas, as is discussed in section 3, the plasma-line scattering is much less so, if at all. For purposes of this comparison let us assume no aspect sensitivity for the plasma-line scattering. As shown in section 5, the east-west extent of the heated volume was sufficiently great that beam filling in azimuth at both VHF and UHF was fulfilled. With regard to the other dimensions, it is seen from the results in section 3 that the plasma-line scattering takes place in a region above the heater relatively narrow in altitude extent. Hence the difference between the VHF and UHF vertical beamwidths does not contribute to a difference in the sizes of the per-pulse plasma-line scattering volumes. The remaining parameter is the pulse width which, as shown in Table 1, was three times longer at VHF. However, since the altitude extent of the scattering region is not precisely known, it is not clear exactly what the scaling with the pulse width should be. Let us minimize the difference between the VHF and UHF scattering volumes by ignoring the difference in the pulse widths. Then the per-pulse scattering volume at VHF is larger than the UHF per-pulse volume by a factor of at least 435/157.5 or 4.5 db which, added to the 7 db difference in the values for σ_T gives a difference of at least 11 db. To summarize, therefore, we have the situation that, for the center line, the per-unit-volume backscatter cross section is 7 db greater at VHF than at UHF, whereas for the plasma line the per-unit-volume backscatter cross section is at *least* 11 db greater at UHF than at VHF.

This reversal in frequency dependence of the scattering properties of the two modes is unexpected and striking. It would be interesting to have data at additional frequency points in order to determine how high in frequency this reversal extends, where the maximum is, etc. Unfortunately the next highest frequency available for these experiments was 1300 MHz (AMRAD) at which neither center-line nor plasma-line backscatter was ever observed. For the UHF plasma-line scattering there is an additional possibility. Because as discussed in section 3.2 the aspect sensitivity is much weaker, the scattering lobe width may be correspondingly much broader than for the center line. But the peak backscattered power in both cases is observed to be essentially the same. Hence it is possible at UHF that, for the plasma line, the total scattered power may be considerably greater than for center-line scattering. At VHF there is virtually no such possibility because of the great difference in the backscattered power levels between the two modes.

3. ASPECT SENSITIVITY AND LONGITUDINAL SCALE SIZES

3.1. *Center line.*

3.1.1. *Aspect sensitivity.* At the beginning of these experiments it was generally expected that the center-line scattering would also be associated with plasma waves produced by parametric instabilities, and that the major factors determining the location of the scattering region for *o*-mode excitation would therefore be essentially described by the Bohm-Gross dispersion relationship:

$$\omega_h^2 = \omega_p^2 + 3k_w^2(KT_e/m) = \omega_p^2(1 + 3k_w^2 D^2) \quad (1)$$

together with the requirement $0 < k_w D < 1/4$, outside of which the waves suffer large Landau damping [*Perkins et al.*, 1974]. In these expressions, $\omega_h = 2\pi f_h$, $\omega_p = 2\pi f_p$, k_w is the plasma wave number, KT_e/m is the square of the electron thermal velocity, and D is the electron Debye length. The criterion $k_w D < 1/4$ limits the thickness of the region to 10 km and the lower wavelength limit to about 8 cm; for any given wavelength, the altitude extent is further restricted to the order of 1 km. It was therefore originally expected that the heating effects would be observed to be confined to a quite thin nominally horizontal layer centered at the altitude where $\omega_h \simeq \omega_p$ (the factor $(3k_w^2 KT_e/m)^{1/2}$ is of the order of a few kHz). As discussed in section 2 however, it was found instead that the overall effects of the heating for purposes of producing VHF/UHF scattering are in fact quite spread out in altitude extent ($\gtrsim$40 to 50 km), and that the actual region within which scattering from one particular location to another takes place is dominated by the scattering geometry relative to **B**.

The fact that for center-line scattering the aspect

sensitivity is so extreme, with the perpendicularity condition being in fact essential for backscatter, was first discovered as the result of an experiment carried out to determine the location of the scattering region within the heated volume. In this experiment the variation with slant range of the scattering point of the radar echo was measured as a function of the RAM elevation angle, α. Referring to Figure 3 it is seen that, for small total ranges of the elevation angle scan, if the scattering region is effectively planar, then the variation of the elevation angle with range will be a constant, $\tan \phi/R$, from which the orientation, ϕ, of the locus of points of maximum scattering within the plane containing RAM and the heater can be obtained by: $\tan \phi = R\Delta\alpha/\Delta R$. We also note from Figure 1, that for elevation scans around the perpendicular point over the heater, for which the elevation angle is nominally 15°, the value of ϕ for a horizontal scattering layer is 22°.

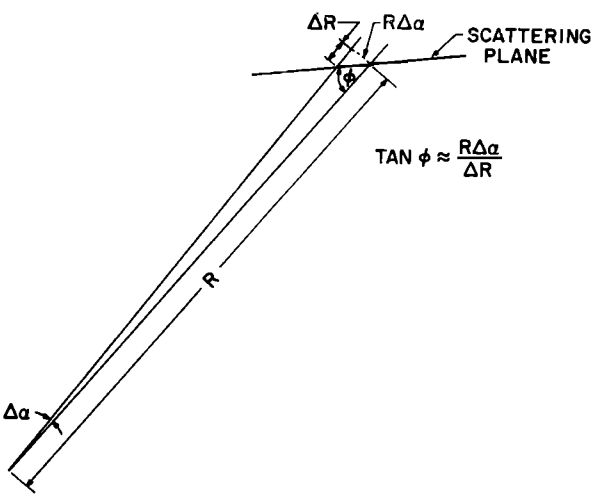

Fig. 3. Determination of orientation of the scattering region from the elevation-scan experiment. For a planar region a constant slope of angle versus range, $\Delta\alpha/\Delta R$, is observed.

This experiment was first carried out in October 1971. Both VHF and UHF results were obtained; however, the results are more easily interpreted at UHF because of the narrower antenna beamwidth. A Range-Time-Intensity (RTI) presentation of one of these results is shown in Figure 4. It is seen that the slope of angle vs. range is quite well defined, clearly indicating a planar scattering region. For these data the elevation scan rate was 0.5° sec^{-1}, from which we find for $\Delta\alpha/\Delta R$, the slope of the locus of points of maximum backscatter through the center of scattering region in the RTI, a value of .625/37 deg per km. But, taking the range to the perpendicular point over the heater to be 925 km, we find the value of ϕ to be 15.2° rather than 22°. Hence, rather than being horizontal, the scattering region is seen to be inclined to the horizontal by about 7°, the southern end being lower than the northern end. For the magnetic field geometry in these experiments such a tilt in this direction obviously brings the radar **k** vector more nearly into perpendicularity with the magnetic field across the extent of the scattering region. The next step in the analysis of the data was to plot the location of the observed scattering region using the measured values of R and α, in order to determine the angle between the radar line of sight and the direction of **B** at each of the points defining the locus of maximum backscatter as determined from the RTI. In this analysis a constant value of 68° for the magnetic dip angle was assumed across the heated volume. The results of this calculation for the RTI shown in Figure 4 are presented in Figure 5. It is seen that, over the range of elevation angles, at each point of intersection between the radar line of sight and the locus of maximum scattering the line of sight is very close to perpendicularity to **B**, with the maximum difference, at the southernmost point, being 1.6°. These differences from perpendicularity are well within the uncertainty in the true direction of **B** which resulted from the use of a constant dip angle. Let the perpendicularity contour, $C_\perp$, be defined as the locus of points over which the radar line of sight is perpendicular to **B**. It is also seen from the figure that the angle between $C_\perp$ and the horizontal as calculated under the assumption of a constant 68° dip angle, is very close to 7°. Analysis of additional elevation scan data from these experiments shows almost exactly the same results. From this we conclude that maximum backscatter takes place along the locus of points within the heated volume where the radar line of sight achieves perpendicularity to **B**, and that the small differences between the calculated values and 90° in this case are due to the rough magnetic field model used in the calculations. This conclusion receives further confirmation by replotting the data on a more accurate perpendicularity contour [*Thome and Blood*, 1974] using a 99-term spherical-harmonic expansion of the geomagnetic field.

The experimental results therefore show the scattering region to be centered on $C_\perp$. The true thickness of the scattering region, on the other hand, cannot be determined from these experiments. As is discussed by *Minkoff* [1973*a*, *b*], although the dimensions of the

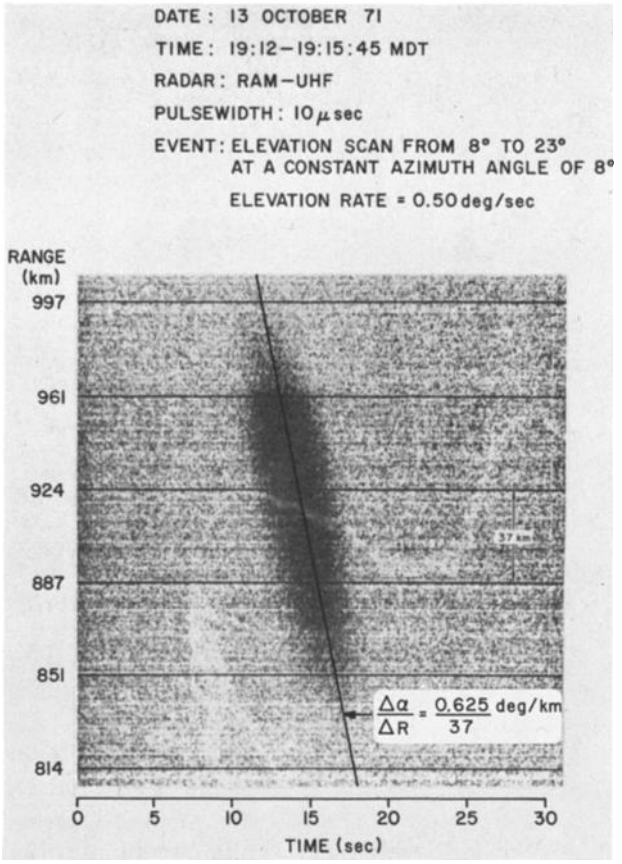

Fig. 4. Results of UHF elevation-scan experiment indicating a planar scattering region. The straight line in the figure essentially coincides with $C_\perp$. Regarding the shape of the RTI, the width of the R versus α plot, along any horizontal line defined by fixed R, is described by equations 3 and 4. Since $L > D$ (see section 3.1.1), the width is determined essentially by the antenna beamwidth.

heated volume may be arbitrarily large, because of the aspect sensitivity, backscatter is actually produced over a distance, which is most conveniently measured along the direction of B, of the order of $\lambda R/2L$. Thus, measurement of the true thickness of the scattering region is in fact equivalent to measuring the aspect sensitivity of the scattering which, as discussed in the above references, is limited by the resolution capability of the radar system. As a result, all such observed quantities whose magnitudes are dependent on the aspect sensitivity of the scattering will, unless the appropriate resolution requirements are satisfied, turn out to be determined by the parameters of the radar systems by which the measurements are made rather than by the ionospheric scattering properties themselves. Experimental demonstration of this is given in section 3.1.2.

3.1.2. *Longitudinal scale sizes.* The extreme aspect sensitivity of the center-line scattering is reminiscent of the radio aurora for which a per-unit-volume differential cross section has been derived by *Booker* [1956] which we write in the form

$$\sigma = r_e^2 \langle |\Delta n|^2 \rangle S_L S_T \qquad (2)$$

where r_e is the classical electron radius e^2/mc^2, $\langle |\Delta n|^2 \rangle$ is the variance of the electron density fluctuations, and it is assumed that the spatial wave number spectrum of the electron density distribution, S, can be written separately in terms of a longitudinal and a transverse part, S_L and S_T, which describe respectively the spatial frequency content of the electron density distribution parallel and perpendicular to B. The quantities S_L and S_T are in turn characterized by the longitudinal and transverse coherence lengths or scale sizes, L and T, which can be interpreted as the average distances parallel and perpendicular to B over which collective scattering effects take place. For the case of significant aspect sensitivity of interest here we have $L/T \gg 1$; for this condition arguments justifying writing the spectrum in separable form, $S = S_L S_T$, are presented by *Minkoff* [1973*a*].

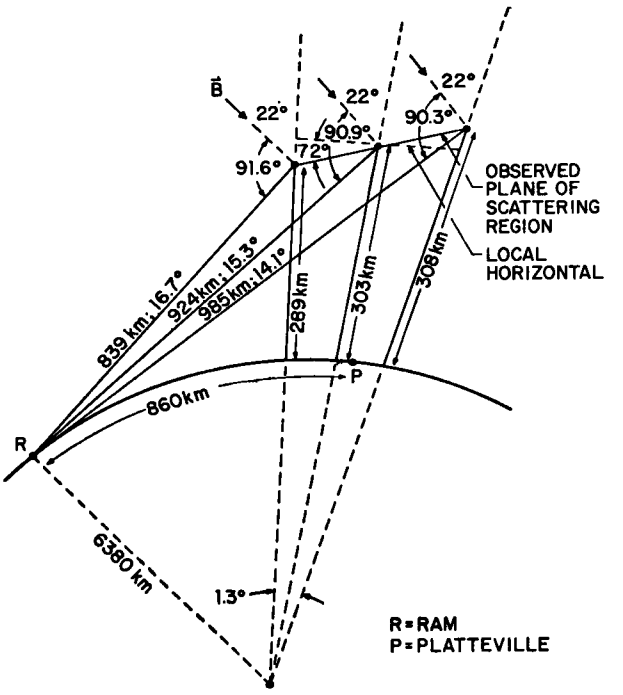

Fig. 5. Results of analysis of experimental measurement shown in Figure 4, determining the orientation of the locus of points of maximum scattering in relation to the direction of the geomagnetic field, B. From these results it was first determined that the locus of points of maximum backscatter for the center-line mode coincides with $C_\perp$.

The aspect sensitivity, or equivalently the angular distribution of the scattering within a plane containing **B**, is described by the function S_L. One might attempt to determine S_L by measuring, at a fixed slant range, the backscattered power as a function of the angle of incidence between the radar line of sight and **B** at the scattering point; similar measurements have been carried out for the radio aurora [*Chestnut et al.*, 1968]. *Minkoff* [1973*a*] has shown that $P_R(\gamma)$, the backscattered power at a fixed range R as a function of γ, the angle of incidence between the radar line of sight and **B**, is given by the expression:

$$P_R(\gamma) = F(k)(1/\theta_\perp) \int_{-\infty}^{\infty} G_\alpha{}^2(\alpha - \gamma)\, d\alpha \cdot \int_{-\theta_\perp/2}^{\theta_\perp/2} S_L(2k\alpha + 2k\eta)\, d\eta \quad (3)$$

where $F(k)$ is a certain function of k which need not be considered further here, $\theta_\perp = \Delta \tan \phi_\perp / R$ where $\phi_\perp$ is the angle between the radar line of sight and $C_\perp$, a rectangular pulse is assumed with $\Delta = c\tau/2$, τ = pulse width, and G_α is the vertical antenna beam pattern. $G_\alpha{}^2(\alpha)$ and $S_L(2k\alpha)$ are characterized by nominal 3-db widths $\delta\alpha \simeq \lambda/2D$ and $\delta\alpha \simeq \lambda/2L$, respectively, where D is the vertical antenna aperture defined in terms of the vertical beamwidth, θ_α, as $D = \lambda/\theta_\alpha$.

However, as discussed by *Minkoff* [1973*a*, *b*], measurement of S_L by this procedure is possible only if $D \gg L$ and $\theta_\perp \ll \lambda/2L$. In these experiments, using $\phi_\perp \simeq 15°$, we have $\theta_\perp \ll \lambda/2D$, in which case the vertical antenna aperture is the limiting factor and (3) becomes

$$P_R(\gamma) = F(k) \int_{-\infty}^{\infty} G_\alpha{}^2(\alpha - \gamma) S_L(2k\alpha)\, d\alpha \quad (4)$$

It is seen from this expression that if $D < L$ the function S_L effectively becomes a delta function, and one actually measures $G_\alpha{}^2$ rather than S_L. As a corollary, if an estimate of L should turn out to be nominally equal to D then from the result one can infer only that the true value of L is greater than or equal to D.

Experimental measurements of $P_R(\gamma)$ were carried out during these experiments a number of times. The experiment was most conveniently performed at RTMS where an incoherent integrator was incorporated into the receiver system thereby providing, in essentially real time, for smoothing of the random time fluctuations in the received signal. The results of such an experiment, carried out in February 1973, are presented in Figure 6. For each value of γ a smoothed pulse echo consisting of an average of 100 individual echoes was obtained from which, at a fixed range of 925 km, the value of $P_R(\gamma)$ was determined. The values of $P_R(\gamma)$ obtained in this way which are shown in Figure 6 are seen to be a very good fit to the square of the vertical RTMS beam pattern, $G_\alpha{}^2$. From this it can therefore be concluded only that L is larger than 85 ft and, from the close fit in Figure 6 between $G_\alpha{}^2$ and the data, probably very much larger. Because of this fundamental limitation on the determination of S_L, and the relatively small sizes of the antennas of the White Sands radars, no more precise determination for L was possible in these experiments.

3.2. *Plasma line.*

By the experiments described in section 3.1.1 it has been found, without exception for all such data which have been examined, that center-line backscatter takes place within a narrow planar region centered on $C_\perp$. For plasma-line backscatter, however, this is not the case. It has been found that plasma-line backscatter cannot always be interpreted as emanating from a planar region, and maximum backscatter does not take place along $C_\perp$. Examples of observations of nonplanar regions for plasma-line scattering are shown in RTI presentations of elevation scans in Figure 7. It is clear from these RTIs that the orientation of the observed scattering region in each case cannot be defined by a straight

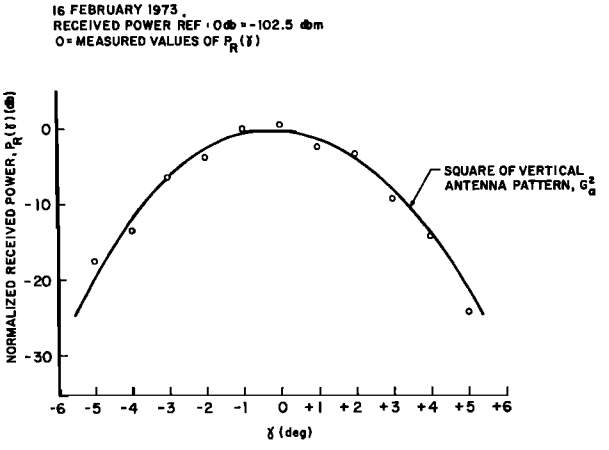

Fig. 6. Result of measurement described by equations 3 and 4. The horizontal scale in the figure has been arbitrarily adjusted so that $P_R(0)$ is the maximum value.

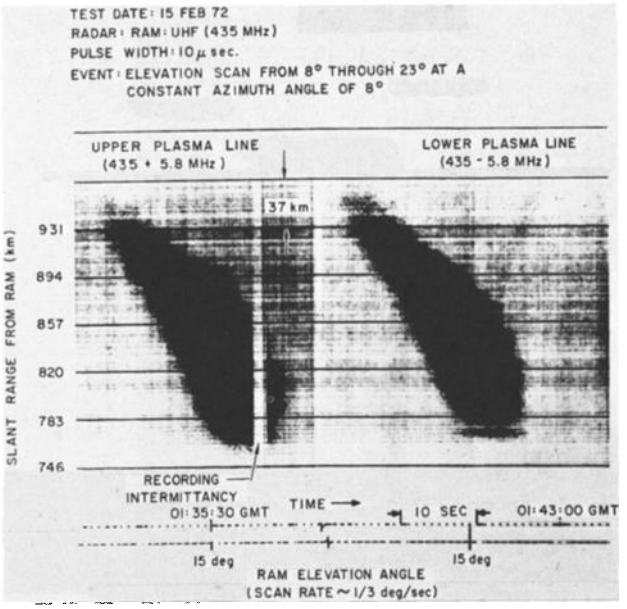

Fig. 7. RTI presentation of results of UHF plasma-line elevation-scan experiment showing nonplanar scattering regions.

line of constant slope and the results therefore do not admit a simple interpretation in terms of a planar scattering region. With regard to the aspect sensitivity, Figure 8 shows RTI presentations of a sequence of elevation scans alternately between the upper and lower plasma lines and the center line. In these cases all the scattering regions appear to be planar, as evidenced by the well-defined slopes of R vs. the elevation angle. However, the values of the slopes are not the same. This is shown clearly in Figure 9 where the locations of the scattering regions for the three scans, as determined from the RTIs of Figure 8, are plotted. For the center line the orientation of the scattering region is seen to coincide very closely with the perpendicularity contour. At this time heating was taking place near 290 km. The plasma-line scattering regions are seen to coincide essentially with h_f at the southern end and fall off progressively with altitude northward; this northward droop for the plasma-line scattering region was observed quite often. It is evident that

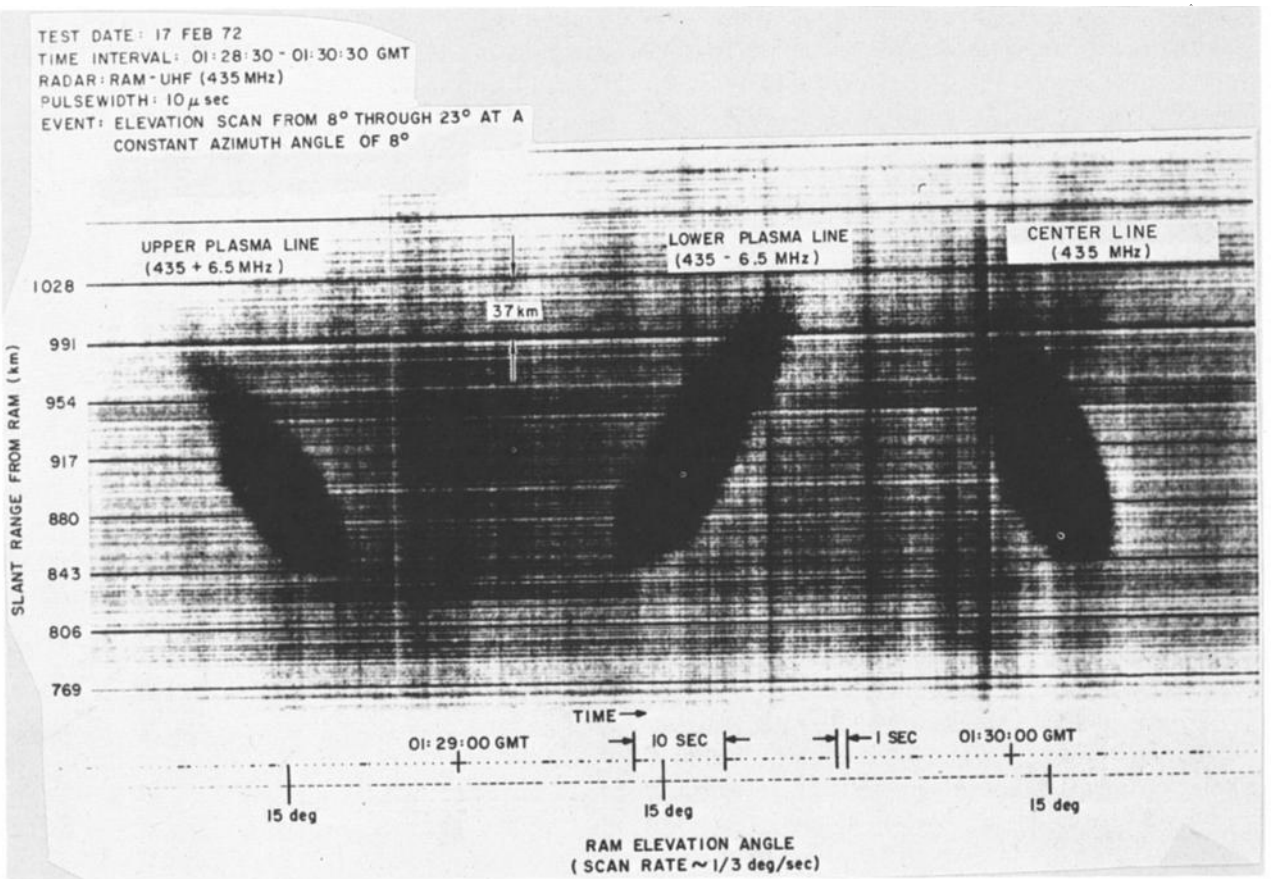

Fig. 8. RTI presentation of continuous sequence of elevation scans for UHF center-line and upper and lower plasma-line scattering. Results indicate planar scattering regions with different slopes.

the plasma-line and center-line scattering regions are distinctly separate. It is also of interest to note that the upper and lower plasma-line regions though parallel do not actually coincide, and do not have the same range extent.

A more extreme case, in which plasma-line backscatter was observed for relatively large angles of incidence to B, is shown in Figure 10. Here the off-perpendicular angles are as much as 6°, for which center-line backscatter was not observed. It is also seen that, as before, the scattering regions coincide quite closely with the estimated heating altitudes h_f. Thus, in contrast to center-line scattering, the plasma line backscatter was obviously maximized by directing the radar line of sight at the nominal altitude where maximum heating was believed to be taking place independently of the geometry relative to B. Although this indicates perhaps a much weaker aspect sensitivity for the plasma-line scattering, the possibility of some degree of aspect sensitivity cannot be completely ruled out since the magnitude of the plasma-line echoes for heating near the perpendicularity point at 290 km above the heater, as shown in Figure 2, bottom, were approximately 20 db greater than for the results shown in Figure 10 (i.e., the signal-to-noise ratio for the UHF echo in Figure 2, bottom, is

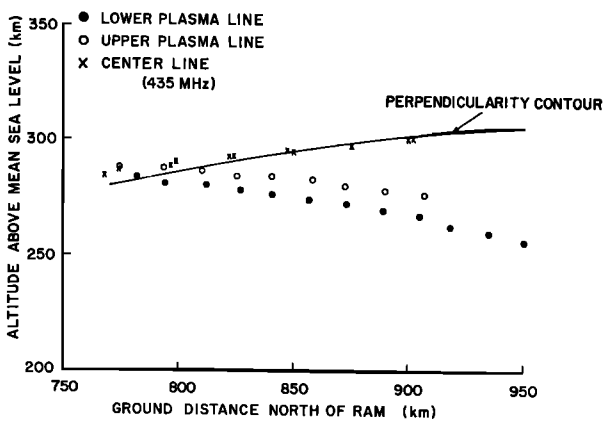

Fig. 9. Locations of loci of maximum scattering for experimental results of Figure 8. The perpendicularity contour, $C_\perp$, shown in this figure was calculated from a 99-term spherical-harmonic expansion of the geomagnetic field [*Thome and Blood*, 1974]. The locus of points of maximum scattering for the plasma-line measurements intersects $C_\perp$ at an altitude of 290 km but is otherwise completely distinct from $C_\perp$. This indicates that (a) plasma-line scattering is much less aspect sensitive than center-line scattering, and (b) the location of the scattering region from the center line is determined by h_f, independently of the geometry relative to B. At this time $h_f \simeq 290$ km.

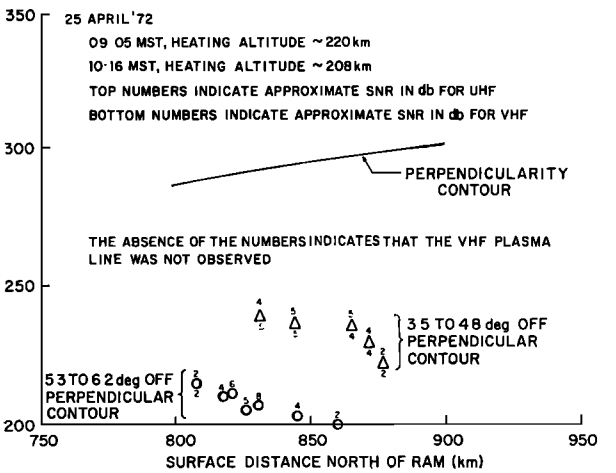

Fig. 10. Location of VHF and UHF plasma-line scattering regions as functions of h_f. No center-line scattering was observed at this time. Note that, consistent with the discussion of section 2.2, the scattering of UHF is stronger than at VHF. Triangles are data points for $h_f \simeq 220$ km. Circles are data points for $h_f \simeq 208$ km.

25 to 30 db). On the other hand, as noted above, heating at 290 km could only be accomplished after sundown because of the high critical altitude required, whereas the results of Figure 10 were obtained during daylight hours in the presence of the *D* layer. Thus it is possible that the weaker echoes in Figure 10 resulted from a reduction in the power of the HF signal at the actual heating altitude owing to *D*-layer absorption. The question of whether or not the plasma-line scattering is aspect sensitive, and if so to what extent, was not resolved by these experiments.

4. TIME-DEPENDENT CHARACTERISTICS

Information concerning the time-dependent behavior of the scattering properties of the heated volume was obtained from spectra of the radar echoes and measurement of the step response of the backscatter cross section to the heater excitation. Spectra for both the center-line and plasma-line returns were obtained by means of periodogram processing of coherently recorded VHF echoes at RAM. From these data the coherence time of the scattering as well as the mean ionospheric drift velocity are determined. The step responses are the measured rise and decay times of the backscatter cross section in response to sudden turn-on and turn-off of the HF heating signal. A detailed report on these observations is currently in preparation. In what follows, a few examples of these results are presented.

An example of a center-line spectrum is presented in Figure 11, top. The spectral width is defined here as the second spectral moment for which the calculated value for this example is 6.7 Hz; the error in this measurement is of the order of ± 2 Hz. The first spectral moment determines the Doppler shift, presumably due to north-south ionospheric drift, with of course a possible ambiguity of $\pm n \times 100$ Hz (n = 1,2,3, . . .) because of the 100-Hz pulse repetition frequency. Assuming no ambiguity, the ionospheric drift in this example was 27.7 m sec^{-1}, southward. It is interesting to note that in these experiments no northward drift was observed over the two-year period.

An example of a plasma-line spectrum is presented in Figure 11, bottom. For the plasma lines, the detection process required an offset of the IF frequency by an amount determined by the HF heater frequency at the time of the observation. Uncertainty both in the knowledge of the exact heater frequency and in the exact IF local oscillator frequency resulted in an uncertainty in the measured value of the plasma-line Doppler frequency of the order of ± 50 Hz, which is too large in comparison with the accuracy in the measurement of the center-line Doppler shift to be of interest for comparison. The spectral width measurement, however, is unaffected by these factors and is seen to be 8.2 Hz with the error being essentially the same as for the center line, ± 2 Hz.

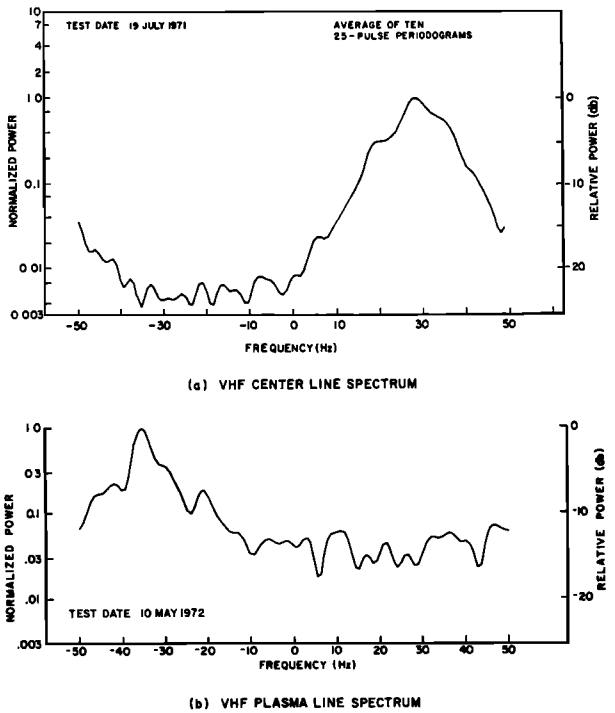

Fig. 11. Center-line and plasma-line VHF spectra obtained from periodogram analysis. The spectral widths in both cases are comparable and quite narrow (6.7 and 8.2 Hz respectively). The frequency offset of 30 Hz for the center line can be interpreted in terms of a southward ionospheric drift of about 30 m sec^{-1}.

The spectra for both scattering modes are therefore seen to be quite narrow, corresponding to a relatively long coherence time of the order of 0.1 sec. For the plasma line the narrow bandwidth is particularly striking in comparison with AIO results where 2-kHz bandwidths are reported. As noted above, this would indicate that the existing theories which explain plasma-line scattering in terms of scattering from plasma waves produced by parametric instabilities [*Perkins et al.*, 1974] and which are quite successful in predicting the observed AIO spectra probably do not apply to these results.

With regard to the rate at which the ionospheric scattering properties are effectively turned on and off by the heating process, an RTI showing the VHF center-line echoes as observed during various on-off modulations of the heater power is presented in Figure 12. In general, at both VHF and UHF and for both scattering modes, large increases—say 10 db—in response to sudden turning on of the heater power were observed in time periods of the order of the RAM interpulse period of 10 msec. As can be seen in the figure, the rate of increase is faster than the rate of decay when the heater is suddenly turned off.

5. SPATIAL CONFIGURATION OF HEATED VOLUME

Extreme differences in the spatial configuration of the heated volume were observed depending on whether f_h/f_oF_2 was greater or less than unity. For $f_h/f_oF_2 < 1$, the horizontal dimensions of the heated volume were found to be quite well defined by the nominal 3-db HF heater beamwidth. Determination of the east-west extent of the heated volume was accomplished with the radars at White Sands by measuring the backscattered power level as a function of azimuth angle, the elevation angle being held fixed. By this procedure it was found that the strength of the heating effects along a nominally east-west axis can be described to a good approximation by the function exp [$-(\phi^2/2\sigma_H^2)$] where ϕ is the angle measured from the perpendicular to the earth's sur-

face at Platteville. At a time when f_h was equal to 4.9 MHz a value of σ_H of 8.4° was measured, corresponding to a 3-db heater beamwidth of 23° which is in very good agreement with reported values [*Utlaut,* 1970] scaled to the heater frequency at the time of this measurement. Along the nominally north-south axis the extent of the heated volume as seen from White Sands was observed to be elongated by perhaps 10 to 20% over the east-west extent which probably occurs, as can be shown from ray-tracing calculations [*Meltz et al.,* 1974], because of the presence of the earth's magnetic field.

For $f_h/f_oF_2 < 1$, the radar echoes from the heated volume appeared typically as shown in Figure 2. It is seen that the overall pulse echoes are smooth and the scattering varies essentially continuously as a function of range. As f_h/f_oF_2 began to exceed unity however, it was observed for both scattering modes that the echoes began to develop an irregular spiked appearance. During the course of these experiments it became apparent that the point of transition from a smooth echo to an echo containing irregular spikes provided a relatively precise measure of whether f_h/f_oF_2 was less than or greater than unity, which was sometimes more difficult to determine using ionogram records because of spreading out of the ionogram traces due to the effects of the heating [*Utlaut and Violette,* 1974]. As f_h/f_oF_2 increased further beyond unity large gaps or holes were observed to develop in the central region, denoting absence of, or at least reduced, heating effects. An extreme case of this is shown in Figure 13 where the northern and southern extremes of the heated volume were observed to be completely separated. On interesting example of a hole confined to the central portion of the heated volume is shown in Figure 14. The azimuthal bearing to the center of the hole is 9° and the slant range is 915 km, which for a 15° elevation angle places the hole almost directly above the heater.

Such effects are evidently due to absence of sufficient turbulence to produce VHF/UHF scattering because of penetration of the transmitted HF signal, where the vertical rays directly over the heater penetrate first when f_h/f_oF_2 just exceeds unity. Since for rays propagating off-vertical, the effective ionospheric critical frequency is increased by a factor of the secant of the off-vertical angle, the rays closer to the periphery of the heater beam begin to penetrate only as f_h/f_oF_2 increases further. This is borne out by the fact that in Figure 14 the estimated

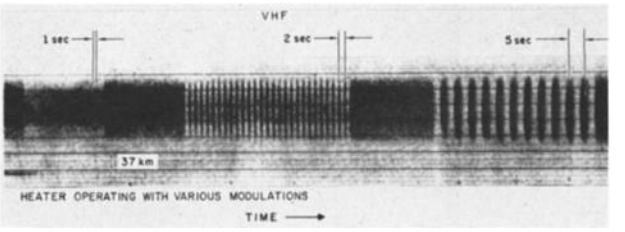

Fig. 12. VHF RTI showing time-response of scattering cross section to various on-off square-wave modulations of heater power.

value of f_h/f_oF_2 is only slightly above unity and, correspondingly, the penetration region is quite small and confined to the central portion of the beam, whereas the large gap in Figure 13 occurs when f_h/f_oF_2 is comparatively large. For f_h/f_oF_2 too much greater than unity the penetration of the heating wave was of course complete and no scattering was observed at all.

In addition to penetration effects, for $f_h/f_oF_2 > 1$ the configuration of the heated volume was observed to become further altered by a mechanism which apparently distinguished between the north-south and east-west axes. The orientation of this nonisotropic distortion of the observed scattering volume suggests that the earth's magnetic field plays a part. In particular, in Figure 13 it is seen that penetration of the heating wave occurs more readily at the eastern and western extremes of the heater antenna beam

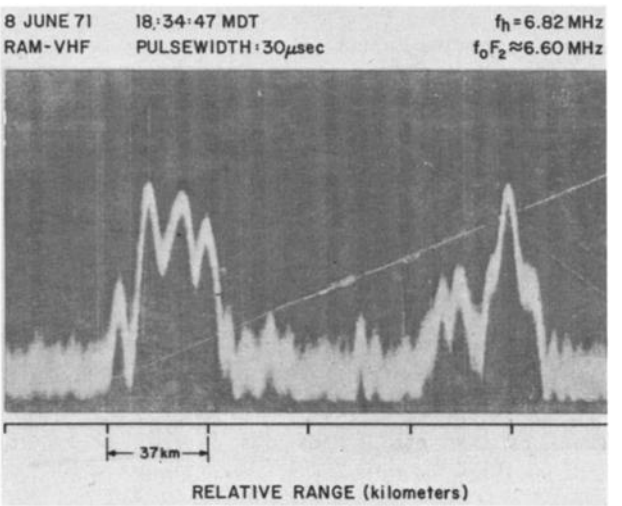

Fig. 13. A-scope record of VHF radar echo for $f_h/f_oF_2 > 1$. The fact that penetration occurs more readily at the eastern and western extremes of the heater beam rather than at the northern and southern extremes may be due to the presence of the earth's magnetic field.

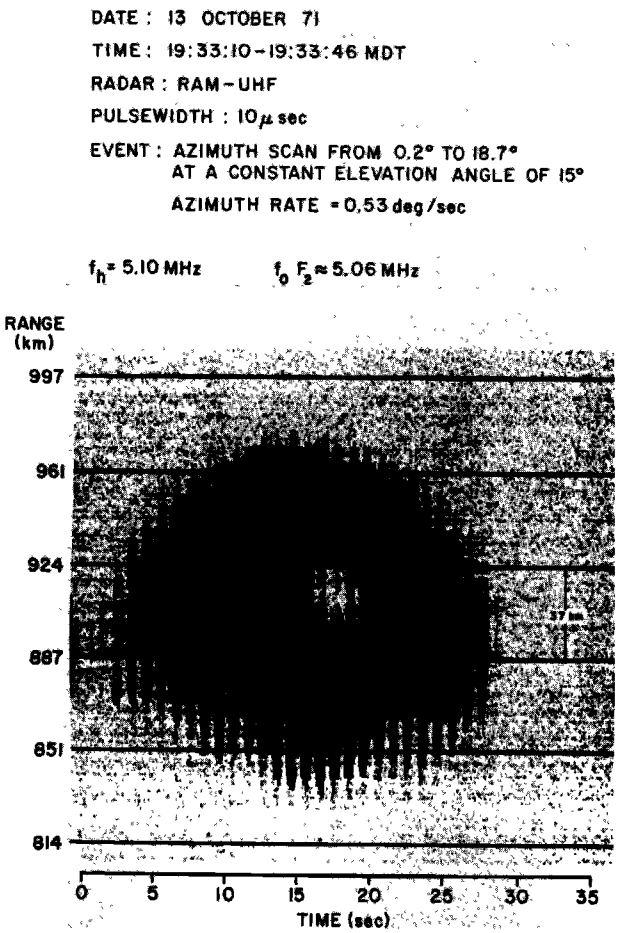

Fig. 14. RTI of azimuth scan of heated volume at fixed elevation angle (the periodic intermittencies in the figure result from a 5-Hz on-off square-wave modulation of the heater power and do not bear on this discussion). Since f_h/f_oF_2 is only slightly greater than unity, penetration occurs in the central region of the heater beam only.

than at the northern and southern extremes. In addition, for $f_h/f_oF_2 > 1$ the scattering volume was observed to become significantly spread out, evidently due to refraction, far beyond the limits set by the normal HF heater antenna beam pattern. The scattering regions at these times were generally observed to consist of one or two strips, narrow in range extent, significantly spread out along an east-west axis. The position in range of these strips coincided nominally with the "normal" northern and southern boundaries of the heated volume as observed for $f_h/f_oF_2 < 1$; as noted, sometimes only one of these strips was observed. Figure 13 can be considered as a projection in the WSMR-Platteville plane of the scattering volume as observed at these times. No such spreading to the north or south was ever observed. Unfortunately, however, these observations were made using center-line scattering only, for which north-south spreading could have been obscured by aspect sensitivity, and the possibility of spreading in this direction therefore cannot be completely ruled out. However, if the spreading were in fact along an east-west direction only, this asymmetry could be due to the presence of the earth's magnetic field and possibly related to the asymmetrical penetration effects discussed in connection with Figure 13. A complete understanding of these observations requires a ray-tracing analysis.

A comparison of the east-west extent of the heated volume for $f_h/f_oF_2 \gtrless 1$ is shown in Figure 15. It is seen that for $f_h/f_oF_2 > 1$ the east-west dimension of the heated volume has increased by approximately 50%. The spreading is eastward only, toward decreasing f_oF_2. As noted, the spread-out portion was also generally observed to become extremely narrowed in range extent, and often appeared on an A-scope presentation as a narrow spike. It was usually found that the radar cross sections of such spikes were quite large and could approach maximum values. In Figure 15, bottom, it is also seen that two maxima occur, at azimuth angles of 6° and 13°. The first of these represents a shift westward of the normal maximum, which was usually observed at 8° and, for evening hours, represents a shift in the direction of increasing f_oF_2. In general the initial penetration effects such as irregular spiked A-scope traces, which were associated with $f_h/f_oF_2 \simeq 1$, were always found to dissappear with an approximate 2 to 3° westward azimuthal antenna shift,

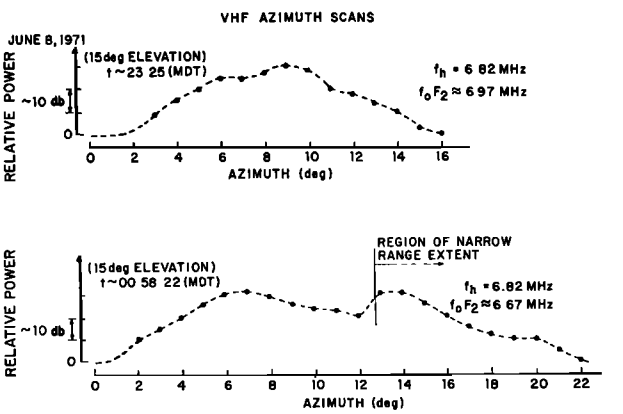

Fig. 15. Illustration of observed east-west spreading of heated volume for $f_h/f_oF_2 > 1$. Note the second peak at 13° in the lower figure, for which radar line of sight was exactly in the plane of the magnetic meridian.

at which point the radar echo was observed to recover its "normal" appearance. The peak at 13° in Figure 15, bottom, is less easy to understand; however, it is to be noted that for this azimuth heading the radar line of sight lies exactly in the plane of the magnetic meridian, which may play a part in explaining the presence of this second peak.

Acknowledgments. We wish to express our appreciation for the cooperation throughout these experiments of E. Violette and J. Carroll of ITS. We would also like to thank the White Sands Missile Range, the US Air Force SAMSO, and the MEWTA organization at WSMR for their cooperation. We also wish to thank R. Kreppel and R. Monroe who contributed to the processing and analysis of these data.

The research presented in this report was supported by the Advanced Research Projects Agency of the Department of Defense and was administered by the Air Force's Electronic Systems Division under contract F19628-71-C-0162.

REFERENCES

Booker, H. G. (1956), A theory of scattering by nonisotropic irregularities with application to radar reflections from the aurora, *J. Atmos. Terr. Phys., 8,* 204–221.

Carpenter, G. B. (1974), VHF and UHF observations of a region of the ionosphere modified by a high power radio transmitter, *Radio Sci., 9,* this issue.

Carroll, J. C., E. J. Violette, and W. F. Utlaut (1974), The Platteville high power facility, *Radio Sci., 9,* this issue.

Chestnut, W. G., J. C. Hodges, and R. L. Leadabrand (1968), Auroral backscatter wavelength dependence studies, *Rep. Proj. 5535,* Stanford Research Institute, Palo Alto, California.

Fialer, P. A. (1974), Field-aligned scattering from a heated region of the ionosphere—Observations at HF and VHF, *Radio Sci., 9,* this issue.

Gordon, W. E., and H. C. Carlson, Jr. (1974), Arecibo heating experiments, *Radio Sci., 9,* this issue.

Meltz, G., L. H. Holway, Jr., and N. M. Tomljanovich (1974), Ionospheric heating by powerful radio waves, *Radio Sci., 9,* this issue.

Minkoff, J. (1973*a*), Analysis and interpretation of aspect dependent ionospheric radar scatter, *J. Geophys. Res., 78* 3865–3879.

Minkoff, J. (1973*b*), Fundamental limitations on aspect sensitive ionospheric scattering measurements, *J. Geophys. Res., 78,* 8399–8401.

Minkoff, J. (1974), Radio frequency scattering from a heated ionospheric volume, 3, Cross section calculations, *Radio Sci., 9,* this issue.

Minkoff, J., M. Laviola, S. Abrams, and D. Porter (1974), Radio frequency scattering from a heated ionospheric volume, 2, Bistatic measurements, *Radio Sci., 9,* this issue.

Perkins, F. W., C. Oberman, and E. J. Valeo (1974), Parametric instabilities and ionospheric modification, *J. Geophys. Res., 79,* 1478–1496.

Thome, G. D., and D. W. Blood (1974), First observations of RF backscatter from field-aligned irregularities produced by ionospheric heating, *Radio Sci., 9,* this issue.

Utlaut, W. F. (1970), An ionospheric modification experiment using very high power, high frequency transmission, *J. Geophys. Res., 75,* 6402–6405.

Utlaut, W .F., and E. J. Violette (1974), A summary of vertical incidence radio observations of ionospheric modification, *Radio Sci., 9,* this issue.

Yngvesson, K. O., and F. W. Perkins (1968), Radar Thomson scatter studies of photoelectrons in the ionosphere and Landau damping, *J. Geophys. Res., 73,* 97–110.

Wong, A. Y., and R. J. Taylor (1971), Parametric excitation in the ionosphere, *Phys. Rev. Lett., 27,* 644–647.